

PAPER • OPEN ACCESS

## QCD Critical point from a black hole engineered EoS

To cite this article: Israel Portillo 2018 *J. Phys.: Conf. Ser.* **1024** 012015

View the [article online](#) for updates and enhancements.

### Related content

- [QCD critical point and correlations](#)  
Mikhail Stephanov
- [Susceptibilities from a black hole engineered EoS with a critical point](#)  
Israel Portillo
- [Strongly coupled quark gluon plasma in a magnetic field](#)  
D A Fogaça, F S Navarra and S M Sanches Jr

# QCD Critical point from a black hole engineered EoS

**Israel Portillo**

Department of Physics, University of Houston, Houston TX 77204, USA.

**Abstract.** We construct an holographic model to map the fluctuations of baryon charge in the strongly coupled quark gluon plasma into a gravitational problem involving the charge fluctuations of holographic black holes. This holograph approach successfully reproduces the baryon number fluctuations calculated on the lattice at zero  $\mu_B$  and makes new quantitatively predictions of those fluctuations at arbitrary  $\mu_B$ . The model displays a critical end point that is located within the reach of the next generation heavy ion experiments.

## 1. Introduction

Exploring the phase diagram of QCD at extremely high temperatures ( $T$ ) and baryonic chemical potential ( $\mu_B$ ) is a prime goal of heavy ion experiments at the Relativistic Heavy Ion Collider at BNL and the Large Hadron Collider at CERN. An important feature of the QCD phases is the line that separates the low- $T$  hadronic matter from the high- $T$  quark-gluon-plasma (QGP). First principles lattice QCD calculations have found that this transition is a rapid crossover at zero  $\mu_B$  [1]. This crossover is expected to become a first order transition at a critical end point (CEP). The existence and location of the CEP is a fundamental question subject of intense study in present heavy ion experiments and one of the main motivations for the construction of the Facility for Antiproton and Ion Research, at GSI. Unfortunately, lattice QCD calculations cannot be performed at finite  $\mu_B$  due to the fermion sign problem and, to guide the experimental search for the CEP in heavy ion experiments, effective approaches must be used.

In this contribution we summarize the results obtained in Ref. [2] with a model constructed using the holographic gauge/gravity correspondence [3], a well-known tool developed in string theory that has been successfully used to study properties of the strongly interacting QGP at finite density [4, 5].

## 2. Holographic Black Hole Model

The action of the holographic model is given by [6, 7]

$$\mathcal{S} = \frac{1}{16\pi G_5} \int dx^5 \sqrt{-g} \left[ \mathcal{R} - \frac{1}{2}(\partial_M \phi)^2 - V(\phi) - \frac{1}{4}f(\phi)F_{MN}^2 \right]. \quad (1)$$

where  $\mathcal{R}$  is the Ricci tensor,  $\phi$  is a scalar field coupled to the metric  $g_{\mu\nu}$ , and  $A_N$  is a Maxwell field, which introduces the baryonic charge effects through the Maxwell tensor  $F_{MN} = \partial_M A_N - \partial_N A_M$ . The non-conformal behavior of the model is controlled by a scalar potential  $V(\phi)$ , used to fix the thermodynamics of the model at zero  $\mu_B$ . Another input parameter is the function  $f(\phi)$ , which corresponds to the coupling between  $A_N$  and  $\phi$ . This function determines the response of the system to a finite  $\mu_B$ .  $V(\phi)$  and  $f(\phi)$  are constructed in such a way that the black hole

model reproduces two crucial observables obtained from lattice QCD calculations at zero  $\mu_B$ : the entropy density ( $s$ ) and the second order baryon density ( $\chi_2$ ) respectively. Therefore, every other observable calculated with this model is a prediction of our model. For instance, Fig. 1 (left) shows the agreement at zero  $\mu_B$  between the trace anomaly of the black hole model and the one calculated on the lattice. The right panel of this figure also shows  $\chi_2$  computed in the black hole model considering three different sets of parameters for  $f(\phi)$  (see Ref. [2] for details). The best fit of the model corresponds to the solid line. The other two sets of parameters take into account the uncertainty coming from the lattice calculation of  $\chi_2$  in Ref. [8] in order to estimate the sensibility of the CEP to the  $T$ -dependence of  $\chi_2$ .

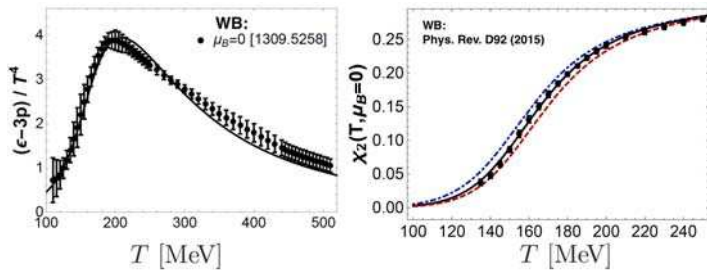


**Figure 1.** Trace anomaly [9] (left) and second baryonic susceptibility [8] (right) from lattice QCD calculations at  $\mu_B = 0$  and compared to our black hole model as a function of temperature.

### 3. Results

The  $n$ -th baryon number susceptibility  $\chi_n = \chi_n(T, \mu_B)$  is defined as  $\chi_n = \frac{\partial^n}{\partial(\mu_B/T)^n} \left( \frac{P}{T^4} \right)$ . Susceptibilities provide essential information about the effective degrees of freedom of a system, and are directly related to the moment of the distribution measured on an event-by-event basis in particle colliders. In the vicinity of a CEP, the susceptibilities  $\chi_n$ 's scale with different powers of the (diverging) correlation length  $\xi$ . One can show that the high order susceptibilities diverge with higher powers of  $\xi$  [10]. In our black hole model, we numerically calculate up to fourth order baryonic susceptibilities at finite  $\mu_B$ , and up to eighth order at  $\mu_B = 0$ .

The black hole susceptibilities are shown in Fig. 2. The error-band on our predictions for  $\chi_6/\chi_2$  and  $\chi_8$  indicates the uncertainty derived by the numerical calculation. One can see that  $\chi_2$  and  $\chi_4$  begin to develop a peak for large chemical potentials, which will then evolve into a divergence at the CEP. The figure also shows the available lattice results for  $\chi_2$  [8],  $\chi_4$  [11] and  $\chi_6/\chi_2$  [12] as a function of  $T$ . Our predictions for  $\chi_4$  and  $\chi_6/\chi_2$ , at zero  $\mu_B$ , have a noticeable agreement with lattice QCD results. As for  $\chi_8$ , our prediction exhibits the expected features from universality [13], which can be compared to future lattice QCD calculations.

Using the higher order susceptibilities calculated at  $\mu_B = 0$ , one can reconstruct the system's pressure  $P$  and baryon density  $\rho_B$  as a Taylor series in powers of  $\mu_B/T$  as follows

$$\frac{P(T, \mu_B) - P(T, \mu_B = 0)}{T^4} = \sum_{n=1}^{\infty} \frac{1}{(2n)!} \chi_{2n}(T) \left( \frac{\mu_B}{T} \right)^{2n}, \quad (2)$$

$$\frac{\rho_B(T, \mu_B)}{T^3} = \sum_{n=1}^{\infty} \frac{1}{(2n-1)!} \chi_{2n}(T) \left( \frac{\mu_B}{T} \right)^{2n-1}. \quad (3)$$

The pressure difference in Eq. (2), and the baryon density in Eq. (3) calculated in the holographic model with no truncations, are compared to the lattice QCD results from Ref. [12] in Fig. 3. The reconstructed holographic pressure truncated at order  $\mathcal{O}(\mu_B^6)$  and  $\mathcal{O}(\mu_B^8)$  is also shown.

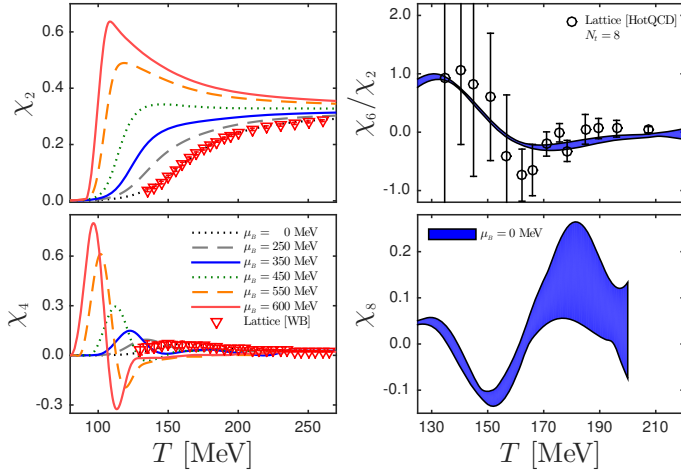


**Figure 2.** Baryon number susceptibilities ( $\chi_n$ ) as functions of the temperature ( $T$ ) for different values of the baryon chemical potential ( $\mu_B$ ) computed using holographic model. The lattice data for  $\chi_2$  and  $\chi_4$  are obtained from Ref. [11], and  $\chi_6/\chi_2$  from Ref. [13].

Our analysis confirms the applicability of the  $\mathcal{O}(\mu_B^6)$  truncation done in [12] for  $\mu_B/T \leq 2$ , and it also predicts that the inclusion of  $\chi_8(T)$  into the expansion extends the domain of applicability of the Taylor series to at least  $\mu_B/T \sim 2.5$ .

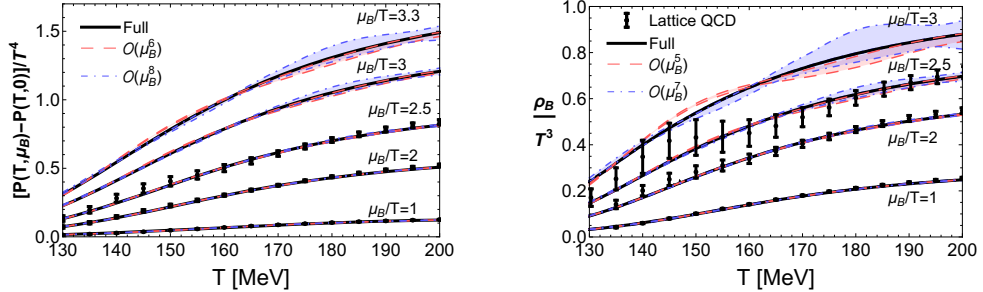


**Figure 3.** The  $\mu_B$ -dependent contribution to the pressure (left) and the baryon density (right) as functions of  $T$  for different values of  $\mu_B/T$ . The solid curves correspond to the full holographic result. The lattice points correspond to the reconstructed Taylor series up to  $\mathcal{O}(\mu_B^6)$  for the pressure and  $\mathcal{O}(\mu_B^5)$  for  $\rho_B$  computed in Ref. [12].

The best set of parameters for the holographic mode is used to calculate  $\chi_2(T, \mu_B)$ , which is plotted in Fig. 4 (left). In the upper plane of the figure, the QCD phase diagram. In order to identify the crossover between hadronic matter and the QGP, we calculate two observables sensitive to this transition: the inflection point of  $\chi_2$  and the minimum in the speed of sound squared  $c_s^2$ , which is shown in the QCD diagram. The CEP is found as divergence in  $\chi_2$  at  $T_{CEP} = 89$  MeV and  $\mu_B^{CEP} = 724$  MeV. Fig. 4 (right) shows the phase diagram with our critical point including the uncertainties from using the three set of parameters in our black hole model. Our CEP is placed inside the region that has not yet been excluded using different approaches [12, 14]. Regions where  $T > 155$  MeV are unlikely to display a CEP due to the known behavior of the curvature of transition line [15].

The chemical freeze-out points, shown in the phase diagram in the upper plane of Fig. 4 (left), were extracted through a comparison of susceptibilities computed in our black hole model and the corresponding net-proton fluctuations from [16] (see Refs. [2, 17, 18] for details). They

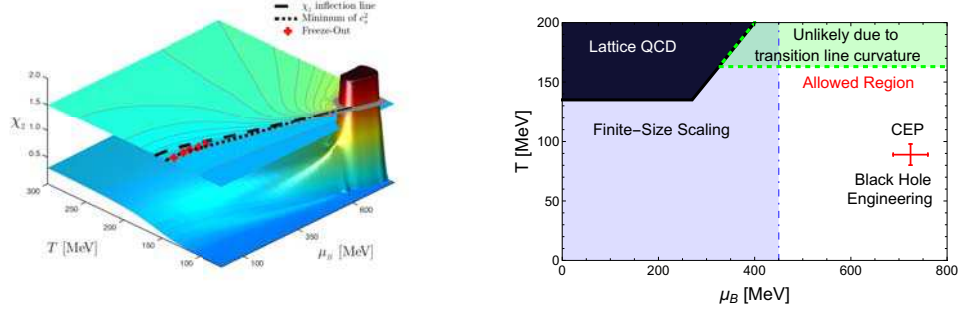


**Figure 4.** (left) Second baryon susceptibility  $\chi_2$  in the  $(T, \mu_B)$  plane determined from the black hole model. (right) Black hole model CEP in the  $(T, \mu_B)$  plane taking into account uncertainties. The shaded areas indicate regions in the QCD phase diagram where the presence of a critical point has been excluded by other approaches.

were found to lie along the transition line defined by the minimum of  $c_s^2$  when  $\sqrt{s} \geq 27$  GeV.

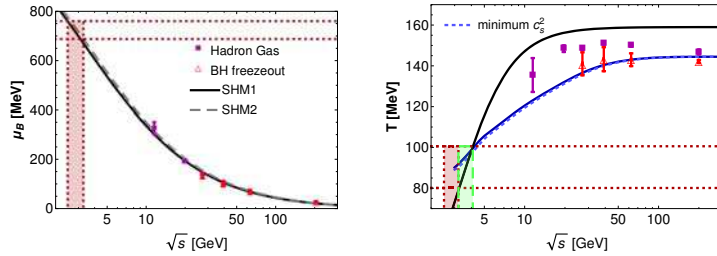


**Figure 5.** Collision energy dependence of the baryon chemical potential (left) and temperature (right) at the chemical freeze-out.

In the following, we extrapolate the behavior of the calculated freeze-out points towards smaller collision energies in order to provide an estimate for the heavy-ion collision center-of-mass energy that could probe the values of  $T_{CEP}$  and  $\mu_B^{CEP}$  found in our black hole model. We use two parametrizations defined using the statistical hadronization model calculations of [19] (SHM1) and [20] (SHM2). Fig. 5 shows both parametrization as a function of  $\mu_B$  (left) and as a function of  $T$  (right). The freeze-out points extracted in the black hole model via a comparison between the  $\chi_1/\chi_2$  and  $\chi_3/\chi_2$ , and those obtained by hadron resonance gas comparisons to net-proton and net-electric charge fluctuations from [21] are also shown in this figure.

By consistently extrapolating this behavior towards smaller collision energies, we find that the CEP of the model could be probed using heavy ion experiments with center-of-mass energy in the range  $\sqrt{s} = 2.5 - 4.1$  GeV.

#### 4. Conclusions

We have used a holographic approach to construct black hole solutions to study the properties of the phases of strongly interacting matter. Our model predicts the existence of a CEP at  $T_{CEP} = 89$  MeV and  $\mu_B^{CEP} = 724$  MeV. Since the CEP is located along the line  $\mu_B/T \sim 8.1$  in the phase diagram, it is beyond the reach of current lattice QCD calculations where  $\mu_B/T \lesssim 2$  [12].

Also, we provide an estimate for the heavy-ion collision center-of-mass energy that could probe the values of  $T_{CEP}$  and  $\mu_B^{CEP}$ . We found that the CEP could be probed using heavy ion experiments with center-of-mass energy in the range  $\sqrt{s} = 2.5 - 4.1$  GeV. These collision energies are within the reach of the HADES experiment [22], the planned Fixed Target (FXT) program also at RHIC [23], and the future Compressed Baryonic Matter (CBM) experiment at FAIR [24].

### Acknowledgments

I thank my co-authors for their collaboration and input in the present proceedings. This material is based upon work supported by the National Science Foundation under Grants No. PHY-1513864, PHY-1654219 and OAC-1531814 and by the U.S. Department of Energy, Office of Science, Office of Nuclear Physics, within the framework of the Beam Energy Scan Theory (BEST) Topical Collaboration. The use of the Maxwell Cluster and the advanced support from the Center of Advanced Computing and Data Systems at the University of Houston are gratefully acknowledged.

### References

- [1] Aoki Y, Endrodi G, Fodor Z, Katz S D and Szabo K K 2006 *Nature* **443** 675–678 (*Preprint* [hep-lat/0611014](https://arxiv.org/abs/hep-lat/0611014))
- [2] Critelli R, Noronha J, Noronha-Hostler J, Portillo I, Ratti C and Rougemont R 2017 *Phys. Rev. D* **96**(9) 096026 URL <https://link.aps.org/doi/10.1103/PhysRevD.96.096026>
- [3] Maldacena J M 1999 *Int. J. Theor. Phys.* **38** 1113–1133 [Adv. Theor. Math. Phys. 2, 231(1998)] (*Preprint* [hep-th/9711200](https://arxiv.org/abs/hep-th/9711200))
- [4] Rougemont R, Noronha J and Noronha-Hostler J 2015 *Phys. Rev. Lett.* **115** 202301 (*Preprint* [1507.06972](https://arxiv.org/abs/1507.06972))
- [5] Rougemont R, Critelli R, Noronha-Hostler J, Noronha J and Ratti C 2017 *Phys. Rev.* **D96** 014032 (*Preprint* [1704.05558](https://arxiv.org/abs/1704.05558))
- [6] DeWolfe O, Gubser S S and Rosen C 2011 *Phys. Rev.* **D83** 086005 (*Preprint* [1012.1864](https://arxiv.org/abs/1012.1864))
- [7] DeWolfe O, Gubser S S and Rosen C 2011 *Phys. Rev.* **D84** 126014 (*Preprint* [1108.2029](https://arxiv.org/abs/1108.2029))
- [8] Borsanyi S, Fodor Z, Katz S D, Krieg S, Ratti C and Szabo K 2012 *JHEP* **01** 138 (*Preprint* [1112.4416](https://arxiv.org/abs/1112.4416))
- [9] Borsanyi S, Fodor Z, Hoelbling C, Katz S D, Krieg S and Szabo K K 2014 *Phys. Lett.* **B730** 99–104 (*Preprint* [1309.5258](https://arxiv.org/abs/1309.5258))
- [10] Stephanov M A 2009 *Phys. Rev. Lett.* **102** 032301 (*Preprint* [0809.3450](https://arxiv.org/abs/0809.3450))
- [11] Bellwied R, Borsanyi S, Fodor Z, Katz S D, Pasztor A, Ratti C and Szabo K K 2015 *Phys. Rev.* **D92** 114505 (*Preprint* [1507.04627](https://arxiv.org/abs/1507.04627))
- [12] Bazavov A *et al.* 2017 *Phys. Rev.* **D95** 054504 (*Preprint* [1701.04325](https://arxiv.org/abs/1701.04325))
- [13] Karsch F 2009 *Prog. Part. Nucl. Phys.* **62** 503–511
- [14] Fraga E S, Palhares L F and Sorensen P 2011 *Phys. Rev.* **C84** 011903 (*Preprint* [1104.3755](https://arxiv.org/abs/1104.3755))
- [15] Bellwied R, Borsanyi S, Fodor Z, Gnther J, Katz S D, Ratti C and Szabo K K 2015 *Phys. Lett.* **B751** 559–564 (*Preprint* [1507.07510](https://arxiv.org/abs/1507.07510))
- [16] Adamczyk L *et al.* (STAR) 2014 *Phys. Rev. Lett.* **112** 032302 (*Preprint* [1309.5681](https://arxiv.org/abs/1309.5681))
- [17] Portillo I 2017 *26th International Conference on Ultrarelativistic Nucleus-Nucleus Collisions (Quark Matter 2017) Chicago, Illinois, USA, February 6-11, 2017* (*Preprint* [1705.01021](https://arxiv.org/abs/1705.01021)) URL <http://inspirehep.net/record/1597600/files/arXiv:1705.01021.pdf>
- [18] Portillo I 2017 *J. Phys. Conf. Ser.* **832** 012041 (*Preprint* [1610.09981](https://arxiv.org/abs/1610.09981))
- [19] Andronic A, Braun-Munzinger P and Stachel J 2009 *Phys. Lett.* **B673** 142–145 [Erratum: *Phys. Lett.* **B678**, 516(2009)] (*Preprint* [0812.1186](https://arxiv.org/abs/0812.1186))
- [20] Cleymans J, Oeschler H, Redlich K and Wheaton S 2006 *Phys. Rev.* **C73** 034905 (*Preprint* [hep-ph/0511094](https://arxiv.org/abs/hep-ph/0511094))
- [21] Alba P, Alberico W, Bellwied R, Bluhm M, Mantovani Sarti V, Nahrgang M and Ratti C 2014 *Phys. Lett.* **B738** 305–310 (*Preprint* [1403.4903](https://arxiv.org/abs/1403.4903))
- [22] Agakishiev G *et al.* (HADES) 2016 *Eur. Phys. J.* **A52** 178 (*Preprint* [1512.07070](https://arxiv.org/abs/1512.07070))
- [23] Meehan K (for the STAR) 2017 (*Preprint* [1704.06342](https://arxiv.org/abs/1704.06342))
- [24] Ablyazimov T *et al.* (CBM) 2017 *Eur. Phys. J.* **A53** 60 (*Preprint* [1607.01487](https://arxiv.org/abs/1607.01487))